Exp Fluids (2012) 52:1465–1474
DOI 10.1007/s00348-012-1267-7

RESEARCH ARTICLE

Investigation of thermal convection in water columns using particle image velocimetry

S. Berthold · C. Resagk

Received: 31 July 2011 / Revised: 9 January 2012 / Accepted: 18 January 2012 / Published online: 7 February 2012

Abstract Particle image velocity measurements were applied on thermally driven convection at low Rayleigh numbers. In a model experiment using a water column heated from bottom and cooled from above, the velocity field was studied at different vertical temperature gradients. In the testing facility with high aspect ratio (about 19) representing a 1-m-long column with 5 cm diameter, occurrence of free convection was verified for destabilizing temperature gradients of 0.1–2 K/m. The PIV results revealed that significant flow exists already at low vertical temperature gradients. The velocity of the stable large-scale circulations increased linearly with temperature gradient (<1 K/m) from 8×10^{-5} to 1×10^{-3} m/s. At higher temperature gradients (1–2 K/m), a transition from quasi-stationary into time-dependent flow was observed, where convection cells changed position, number, and form temporarily. The motivation of this research was to gain more insight into density-driven convection in boreholes and groundwater monitoring wells.

List of symbols

κ	Thermal diffusivity
r	Characteristic length
Ra	Rayleigh number
Ra_c	Critical Rayleigh number
$\Delta T/\Delta z$	Temperature gradient
β	Thermal expansion coefficient
$\tilde{\lambda}$	Ratio of the thermal conductivities of fluid and surrounding material
ρ	Density
v	Kinematic viscosity
g	Gravity of Earth

S. Berthold (✉)
DGFZ Dresdner Grundwasserforschungszentrum e.V.,
Meraner Str. 10, 01217 Dresden, Germany
e-mail: sberthold@dgfz.de
URL: www.gwz-dresden.de

C. Resagk
Institute of Thermodynamics and Fluid Mechanics,
Ilmenau University of Technology, P.O.Box 100565,
98684 Ilmenau, Germany
e-mail: christian.resagk@tu-ilmenau.de
URL: www.tu-ilmenau.de/tfd

1 Introduction

The need to understand thermal convective flow is common to a broad range of geoscience and engineering problems. So the results from very specific applied studies are often valuable for many research areas, like this study, whose results should be generally applicable to thermally driven convection in slender tall water columns.

Motivation for the experimental investigations arose from the fields of hydrogeology and geophysics, where boreholes and groundwater monitoring wells are used to obtain information on rock formation and groundwater properties. As a side effect, boreholes and groundwater monitoring wells create a path that opens up an (additional) possibility of heat and mass transfer between the aquifer under investigation, its surrounding, and the atmosphere. Relevant processes that lead to such transport are vertical convective flows.

Pressure–gradient-induced flows (forced convection) and their adverse impact on hydrogeological, geochemical, and hydraulic measurements have been intensively investigated (e.g., Barczewski et al. 1993; Church and Granato 1996; Martin-Hayden and Robbins 1997; Hutchins and Acree 2000; Elci et al. 2003). The occurrence of free density-driven convection in the water column of

monitoring wells, however, was regarded negligible for a long time (Martin-Hayden 2001). One reason is that the friction forces along the large wall area in the slender geometry (mainly diameters from 5 to 12.5 cm) were thought to hinder the onset of flow.

Theoretical conditions for the onset of free convection are determined through stability analysis based on Rayleigh's theory (Rayleigh 1916), who recognized that free convection can only start if the ratio of the dissipative forces (viscosity and heat/mass diffusion) to the impelling forces (buoyancy) is exceeding a critical value. The dimensionless Rayleigh number describes this ratio, and the critical Rayleigh number describes the state, when convection starts.

For thermally driven convection, the Rayleigh number Ra is defined as:

$$Ra = \frac{\beta g \Delta T/\Delta z}{\kappa \eta} r^4 \quad (1)$$

with thermal expansion coefficient β, gravity of Earth g, temperature gradient $\Delta T/\Delta z$, thermal diffusivity κ, kinematic viscosity v, and a characteristic length r.

Rayleigh's theory, however, was derived for fluid layers, where the influence of the sidewalls is neglected. For vertical channels with circular cross-section, the characteristic length is thus the radius (e.g., Azouni and Normand 1983).

Analytical approximations for the critical Rayleigh number of thermal convection in tall water columns (Ostroumov 1958; Gershuni and Zhukhovitskii 1976; Batchelor and Nitsche 1993) suggest that thermally driven convective flows develop at considerably low temperature gradients in fluid columns.

Numerous experimental investigations of thermal convection have been conducted. However, in former investigations, experimental parameters (e.g., geometry, temperature gradient, mean temperature, or boundary conditions) differed mostly clearly from that expected in groundwater monitoring wells and boreholes. For fluid columns with high aspect ratios (height/diameter), experimental investigations are scarce. Ostroumov (1958) conducted experimental investigations in narrow burettes (0.526–1.0 cm diameter) whose lower part was heated. Sammel (1968) created thermal convection in a 2.75-m-high cylinder (10.2 cm diameter), whose entire lower part was heated and whose upper 1.5-m section was used to measure temperature oscillations. In both studies, the top temperature was not controlled. Azouni (1987) investigated convection cells at temperature gradients of 2.86 K/m and higher in an up to 14-cm-high cylinder (3.5 cm diameter). Arakeri et al. (2000) ran free convection experiments in twelve glass tubes with four diameters (4.85, 9.85, 19.85, and 36.85 mm) and three lengths (150, 300, and 450 mm), where salt water (0.05 g/cm^3) versus distilled water was used to create a density difference. Jerschow (2000) conducted experiments in 3.7-cm-high water columns with a diameter of 0.5 cm applying very high temperature gradients up to 100 K/m.

Yet, their results are not directly transferable to thermal convection in boreholes and monitoring wells under natural temperature and boundary conditions. Major challenges are the associated small temperature gradients. Temperature gradients due to the geothermal gradient are in the order of a few hundredths Kelvin per meter (0.03 K/m on average), and gradients in the near surface zone due to seasonal temperature variations range up to a few Kelvin per meter.

That means, essential prerequisites for a close to reality simulation of natural temperature and boundary conditions are a controlled temperature gradient between top and bottom and an effective insulation of the testing facility against exterior heat influences and heat flux through the walls. The testing facility constructed for the present experiments meets these requirements. It represents a 1-m-long section of a 5-cm-diameter water column with temperature-controlled top and bottom within a temperature-stratified medium.

Due to the small temperature gradients and small geometry, the only reliable way to measure the convective flow is using a non-invasive technique. Thus, for an optimal quantification, particle image velocimetry (PIV) was used. PIV is a non-invasive laser-optical measurement technique that is widely used in flow applications (Raffel et al. 2007). It allows measuring the velocity field with high spatial resolution and without any interference of the flow. Compared with common applications, it is here used to quantify a considerable slow flow.

With the conducted experimental investigations, the following questions are addressed: (1) What is the magnitude of flow velocities induced by very low destabilizing temperature gradients? (2) How does the magnitude change with increasing temperature gradient? (3) What is the characteristic flow structure?

These are important questions regarding vertical thermal convective heat and mass transport in fluid columns as, for example, in boreholes or groundwater monitoring wells. Experimental investigations of thermal convection in water columns with such a high aspect ratio (height/diameter) of around 19 and such low temperature gradients down to 0.1 K/m were conducted for the first time.

Section 2 gives details of the experimental testing facility and provides a description of the PIV setting. Section 3 describes the experimental procedure. Velocity plots have been generated showing the development and geometry of the induced convection cells, as wells as the characteristic flow velocities depending on the destabilizing gradient. The results of the flow measurements are compiled and discussed in Sect. 4.

2 Experiment

2.1 Thermal–hydraulic testing facility

To investigate convective flow in the water column of boreholes or monitoring wells under natural conditions, a medium-scale testing facility was constructed at the Grundwasser-Zentrum Dresden (Berthold 2009). The testing facility represents a 1-m-long section of a water column with 5 cm diameter (approx. 2 inch) in an homogeneous medium (Fig. 1). It allows for applying and maintaining a vertically stratified temperature field with a very low gradient (down to 0.1 K/m) and for optical and thus non-invasive observations and flow measurements (e.g., PIV).

Maintaining a considerably low temperature gradient is a prerequisite for simulating thermal boundary conditions naturally occurring in boreholes and monitoring wells.

Naturally occurring thermal boundary conditions were implemented as follows: Top and bottom of the water column were held at constant temperatures, and along the sidewall of the water column, a linear temperature gradient was created, simulating the heat influx from the surrounding formation.

To achieve high thermal stability, the testing facility was constructed from two interleaved 1-m-long glass cylinders with an inner diameter of 5 and 8 cm and a wall thickness of 0.5 cm, respectively (Fig. 1). Both glass cylinders where tightly sealed at top and bottom through contact pressure each with the help of an o-ring, a PVC carrier disk (2.5 cm high) and a stabilizing stainless-steel disk (0.4 cm high).

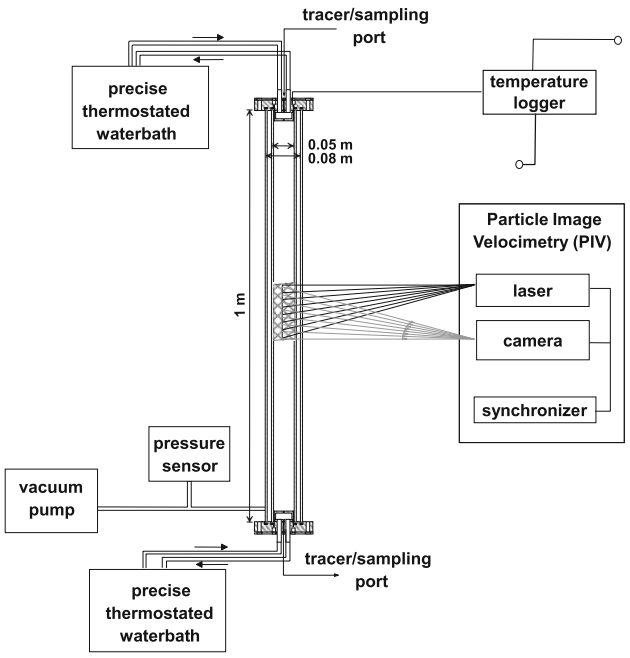

Fig. 1 Sketch of the thermal–hydraulic testing facility

The inner glass cylinder contained the water column, and its ends were formed by two copper chambers (each 2.5 cm high) that were mounted inside the carrier disks (Fig. 2).

The desired vertical temperature gradient was applied to water column and inner glass cylinder (i.e., the water column's sidewall) through the two highly heat-conducting copper chambers at the water column's top and bottom. Heat conductivity of the water column's sidewall (1.13 W/Km) was thereby almost twice the heat conductivity of water (0.6 W/Km). Vacuum in the annulus between inner and outer glass cylinder served as insulation.

In each copper chamber, constant temperature was guaranteed by through flow of tempered water (Fig. 1), provided by a precise thermostated water bath fitted with a circulation pump (Lauda RE 104, temperature stability: ±0.02 K, setting resolution: 0.1 K).

The temperatures and temperature stability inside the water column, the wooden box, and the walk-in box were monitored with temperature sensors. Inside the water column, four sensors were installed at angles of 90°, whose vertical position could be changed along the water column (Fig. 2). Small precise (DIN 1/3B) PT-100 platinum sensors were used (2.2 × 2.3 mm), which could be assessed by a precise 4-channel temperature logger PT-104 (Pico Technology, 0.1°C accuracy, 0.01°C resolution).

In the water column, a verified temperature stability of ±0.025 K was guaranteed by the following constructional elements (Fig. 2): Tempered water was constantly circulated in insulated tubes between the precise thermostated water bathes and the heat-conducting copper chambers. The heat-conducting copper chambers were decoupled from other parts of the testing facility by PVC carrier disks. Vacuum in the annulus between the two glass cylinders insulated the water column against exterior temperature fluctuations.

The whole testing column was housed in a wooden box insulated with hard foam Polystorol. The inner side of the wooden box was tempered with the same water as the upper copper chamber through a copper heating system. The wooden box again was placed in an accessible (walk-in) light-proof box, which was insulated with styrodur, while heat-producing peripheral devices were stored outside.

Two glass windows in the wooden box allowed for optical observation and flow measurements. They could be sealed with Polystorol insulation outside observation periods. For seeding input and water exchange, the water column in the testing facility could be accessed through a small opening (around 1 mm diameter) at top and bottom, respectively.

For flow visualization and quantification, special measurement equipment was installed (Fig. 1), which is described in the following section.

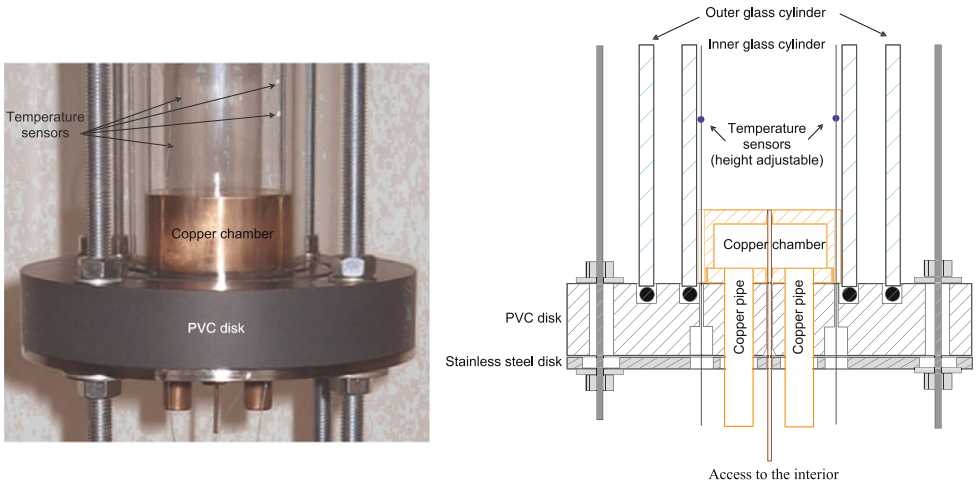

Fig. 2 Details of the testing column with glass cylinders and copper chamber

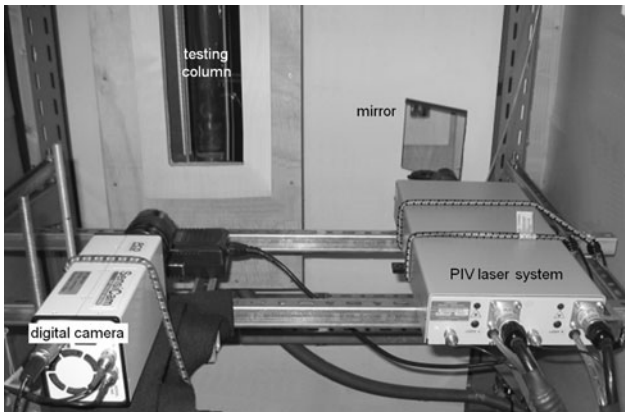

Fig. 3 PIV system with testing column

2.2 PIV system

For quantifying thermally induced free convection in the testing facility, PIV measurements were carried out. PIV measurements utilize a pulsed laser sheet to illuminate special tracer particles, whose positions are then captured using a high-sensitive digital camera (Fig. 3). The non-invasive laser-optical measurement technique simultaneously acquires velocity components in x- and y-directions. A description of the PIV technique, in general, is given in Raffel et al. (2007).

The PIV system used (ILA GmbH) consisted of a laser system (MiniLite PIV) with a double cavity Nd/YAG laser (532 nm wavelength) and a high-sensitive CCD camera (PCO SensiCam) with a resolution of 1,280 by 1,024 pixel. Laser and camera were pulsed synchronously by a synchronizer.

Laser and camera were set up in front of the housed water column. The laser beam was steered to traverse the water column from right to left by a mirror, creating a two-dimensional laser sheet at right angle to the camera lens axis (Fig. 3). The beam had to pass the window in the insulated wooden box—a plane glass plate—and the two interleaved glass cylinders to reach the water column. This complicated optical path resulted in scattering on the glass walls and negligible optical distortions at the margins of the two interleaved glass cylinders (see Sect. 2.3).

Small nylon seeding particles (5 ± 1.5 μm) were used as tracer. They float in water due to their similar density ($\rho = 1.02$ g/cm^3).

2.3 Validation and calibration

Distortion-free determination of the flow field in the PIV images was ascertained using an isogonal reference mesh. The mesh was placed inside the simplified testing facility model and recorded with the PIV camera. The simplified facility was constructed from glass cylinders of identical material, diameters and thicknesses as the original testing facility, but provided easier access. This verification process proved isogonal mapping in nearly all image parts with negligible optical distortions at the margins due to the curved geometry of the two interleaved glass cylinders (Berthold 2009).

2.4 Experimental procedure

To investigate free convection regarding the temperature dependency of convection cell development, cell geometry, and occurring flow velocity, different temperature gradients were realized in the water column (Table 1).

To assure the stated high temperature stability within the water column, temperature at the top of the water column was constantly held close to background temperature (15°C), that is close to the naturally occurring temperature in

Table 1 Parameters of the experiments conducted for flow quantification at different temperature gradients

Run	Bottom temperature (°C)	Top temperature (°C)	Temperature gradient (K/m)	Rayleigh number
1	15.0	15.0	0.0	0
2	15.1	15.0	0.1	355
3	15.2	15.0	0.2	714
4	15.4	15.0	0.4	1,443
5	15.6	15.0	0.6	2,187
6	15.8	15.0	0.8	2,946
7	16.0	15.0	1.0	3,719
8	17.0	15.0	2.0	7,812

the near subsurface (around 10°C). Bottom temperature was set up corresponding to the desired temperature gradient.

The smallest adjustable temperature difference between upper and lower boundary and the temperature steps were limited to 0.1 K by the setting resolution of the water bathes (Lauda RE 104). Accordingly, the experiments were conducted for temperature gradients of 0.1, 0.2, 0.4, 0.6, 0.8, 1, and 2 K/m with temperature increasing downwards.

The thermal Rayleigh numbers for the given experimental parameters (water conductivity: 0.5 mS/cm, pressure: 0 bar) ranged between 0 and 7,812. The explicit values are comprised in Table 1.

After starting an experimental run, a running-in period of at least 14 h guaranteed that temperature and flow regime could adjust optimally to the applied boundary conditions before measurement.

Then, either PIV measurements or long-time exposures were conducted. Owing to the slender geometry and the required high resolution of the PIV images, the PIV field of view was approx. 10 by 10 cm. Thus, the acquired PIV images showed only a section of the water column corresponding to the overall column width and about one-tenth of the overall column height. To capture the complete flow field in the water column, camera and laser sheet were vertically and horizontally (azimuthally) repositioned several times.

At the section of interest, a sequence of 100 PIV images was taken with a predefined time interval (2 or 4 Hz). Repeated sequences of PIV images at the same position allowed for detecting temporal changes and instationarities in the flow field. Sequences in different vertical positions allowed for attaining the flow structure along the water column.

2.5 Velocity field computation and analysis

From the PIV images, the flow field was calculated using the software of the PIV system (ILA GmbH). Owing to the comparatively low flow velocities, the calculation was based not as usual on the two frames of the double-frame PIV images, but on the correlation of the first image frame with the first image frame of the subsequent PIV image.

The process steps applied to the PIV images are summarized in the processing scheme in Fig. 4.

First, the PIV images were calibrated in space and time. For the spatial calibration, that is, to transform the pixel units into real world units, a linear mapping of the images was chosen. In each image, coordinates were provided for four selected points. A ruler installed at one side of the glass column and the glass cylinders wall, which was also observable in the images, served as orientation. The image area was represented by 1,280 × 1,024 pixels. Thereby 1 centimeter in reality corresponded to 120–140 pixels in the PIV image depending on the image sequence.

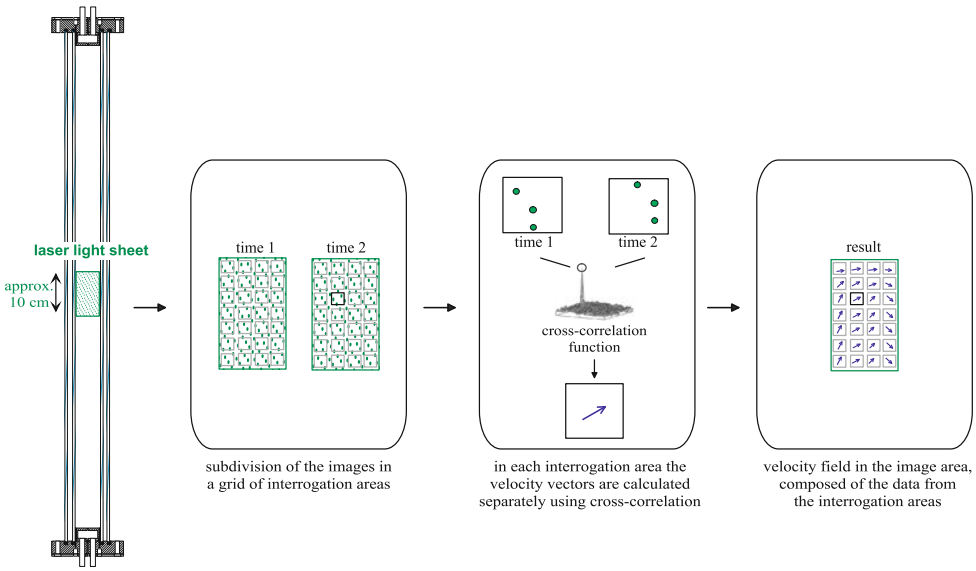

Fig. 4 Field of view and PIV processing schema using the single frame method

The tracer particles with a size of 50 μm were slightly smaller than a pixel (around 71–83 μm) of the PIV image. However, as not the particles are captured, but the scattered laser light in form of an intensity distribution, each tracer particle in the PIV images was represented by several pixels. According to a simple estimation, the percentage of pixels illuminated through scattered laser light within an image was about ten percent.

The following temporal calibration concerned the time interval between two subsequent images. Image frequency was generally 2 Hz. At high temperature gradients with comparatively fast flows, the frequency was raised to 4 Hz.

After conducting spatial and temporal calibration of the PIV images, the velocity vectors were calculated iteratively using cross-correlation analysis. The grid on which the cross-correlation processing was applied was successively refined. In the first step, interrogation area dimension was set to 64 × 64 pixels with an interrogation separation of 64 pixels; that is, there was no overlapping of the individual interrogation areas. An interrogation area corresponded to a quadratic section of the water column with a side length of about 0.45–0.50 cm. For each interrogation area, a velocity vector was calculated from two subsequent PIV images using the cross-correlation function.

Outliers in the calculated velocity field were identified and eliminated through global and local filtering. The global filter detected vectors with too high or too low velocities compared to all velocity vectors in the PIV image. The local filter detected outliers regarding direction and magnitude compared to the eight velocity vectors in the immediate vicinity. The identified outliers were then replaced by interpolated velocity vectors.

In the second and third steps, so-called adaptive cross-correlation was conducted. Adaptive cross-correlation means that the offset between the base and the cross-interrogation area is adaptively chosen close to the local tracer particle displacement (known from the previous cross-correlation analysis). That way data yield (percentage of valid vectors) was considerably improved, and hence, smaller interrogation areas and smaller grid separations could be used, resulting in higher accuracy and higher spatial resolution.

Adaptive cross-correlation with subsequent global and local filtering and interpolation was conducted twice on a successively refined grid. First refinement resulted in an interrogation area dimension of 32 × 32 pixels with an interrogation separation of 16 pixels, and second refinement resulted in an interrogation area dimension of 16 × 16 pixels with an interrogation separation of 8 pixels. In both cases, the interrogation areas were half overlapping.

As final step in data processing, an average flow field was calculated from a sequence of 100 images, corresponding to an average over 25 or 50 s (4- or 2-Hz time interval).

3 Results and discussion

Free convective flow at low Rayleigh numbers was quantified for temperature gradients of 0.1, 0.2, 0.4, 0.6, 0.8, 1, and 2 K/m with temperature increasing downwards (corresponding to Rayleigh numbers from 355 to 7,812). For these temperature gradients, a temperature stability of ±0.025 K was reached within the testing facility. This was only possible by using a complicated insulation system including vacuum around the glass column, interleaved housing, and temperature control.

Secondary heating by the laser PIV technique can be excluded as the measurements were conducted with a 30-mJ pulsed laser with a pulse length of several microseconds, a time between two PIV pulses of several milliseconds and a repetition rate less than 1 Hz.

As expected, water column and hence tracer particles experienced no flow, when no temperature gradient was applied as apparent from the long-time exposure digital photographs (Fig. 5 left). When destabilizing temperature gradients of 0.1–2 K/m were introduced, varying flow patterns were developing (Fig. 5 center and right). Observance and quantification were carried out non-invasively applying PIV.

For temperature gradients of 0.1–1 K/m ($Ra = 355$–3,719), a quasi-stationary large convection cell, comprising almost all the water column, could be observed (Figs. 6, 7). At the upper and lower ends of the large quasi-stationary convection cell, a time-dependent flow developed near the tempered copper chambers (Fig. 7). Its occurrence in the water column of monitoring wells and boreholes, however, is unlikely, as it is most likely due to the restrictive boundary conditions in the testing facility (rigid upper and lower boundaries held at fixed temperatures instead of free boundaries with variable temperature).

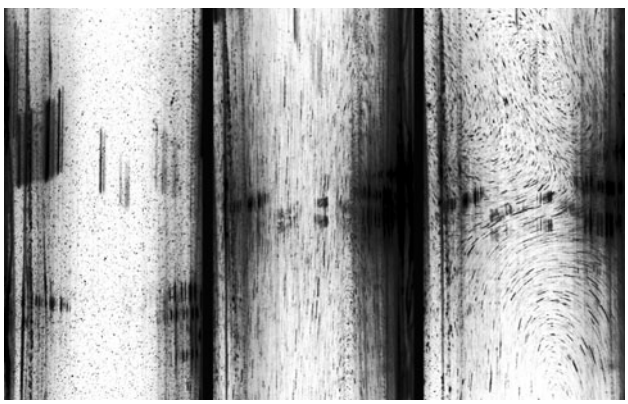

Fig. 5 Long-time exposure of tracer particles in a 5 cm × 10 cm section of the water column; *left*, without temperature gradient; *center*, convection at a temperature gradient of 0.4 K/m; and *right*, at a temperature gradient of 2 K/m

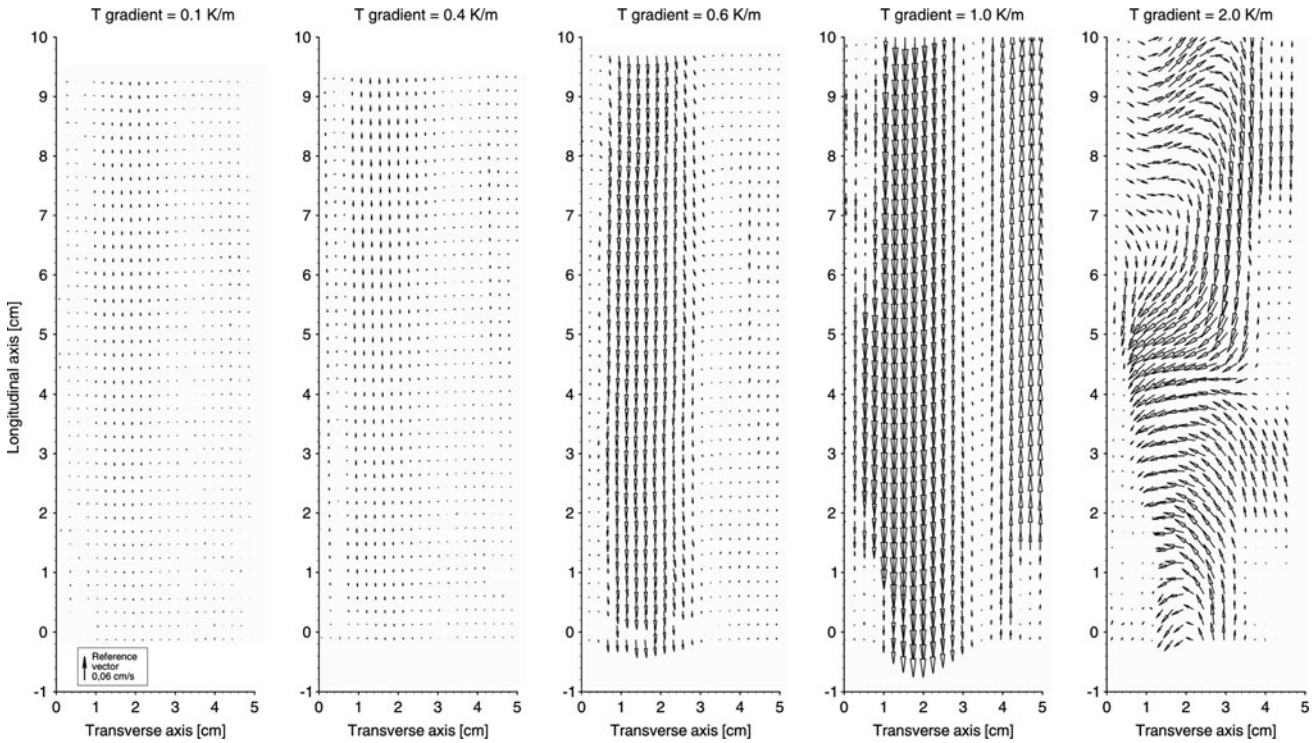

Fig. 6 PIV velocity vector plots of the convective flow in the middle of the water column at temperature gradients of 0.1–2.0 K/m

Flow velocity within the large convection cell was found to increase linearly with increasing temperature gradient for destabilizing temperature gradients between 0.1 and 1 K/m (Table 2). The linear dependency is verified by a high coefficient of determination $R^2 = 0.95$ for a linear regression (Fig. 8). Flow velocities thereby ranged from 8×10^{-5} m/s (7 m/day) for a temperature gradient of 0.1 K/m up to 1.1×10^{-3} m/s (95 m/day) for a temperature gradient of 1 K/m (Table 2).

For a temperature gradient of 2 K/m ($Ra = 7{,}812$), the quasi-stationary large convection was replaced by a time-dependent flow with several convection cells (Figs. 6, 9).

Convection cells changed position in the water column, number and shape with time, partly within a few minutes, resulting in a rather vigorous flow (Fig. 9).

Flow velocity within convection cells caused by a destabilizing temperature gradient of 2 K/m (7×10^{-4} m/s) was surprisingly smaller than at a temperature gradient of 1 K/m (10×10^{-4} m/s). The reason for that decrease in flow velocity is seen in the transition from quasi-stationary to time-dependent flow, leading to a fragmentation into several small convection cells with opposite sense of rotation (Fig. 6). Adjacent convection cells mutually impair each other, thereby.

The finding, that in tall narrow cylinders, a quasi-stationary state characterized by the formation of a single convection cell is established after the onset of free convection, and a transition to time-dependent flow patterns occurs with increasing temperature gradient agrees well with experimental results in short cylinders (e.g., Hales 1937; Azouni 1987).

The presented experimental investigations prove that thermally driven convection occurs in tall, narrow cylinders at considerable low vertical temperature gradients, despite the stabilizing effect of friction forces along the large wall area.

Onset of free convection could be confirmed for temperature gradients down to 0.1 K/m ($Ra = 355$), which was the smallest adjustable constant temperature gradient. Results from earlier numerical modeling compare well with these experimental results. In numerical modeling, a mean velocity of 15×10^{-5} m/s was found for a temperature gradient of 0.1 K/m (Berthold and Börner 2008), and the experimental investigations yielded a mean velocity of 9×10^{-5} m/s.

Both studies prove the existence of thermal convection for temperature gradients down to at least 0.07 K/m (numerical modeling) and 0.1 K/m (experimental investigations), respectively. This is in agreement with an analytical approximation based on a formula of Gershuni and Zhukhovitskii (1976), which proposes that thermal convection should start for a destabilizing vertical temperature gradient of 0.068 K/m in a 5-cm-diameter water column (Berthold and Börner 2008).

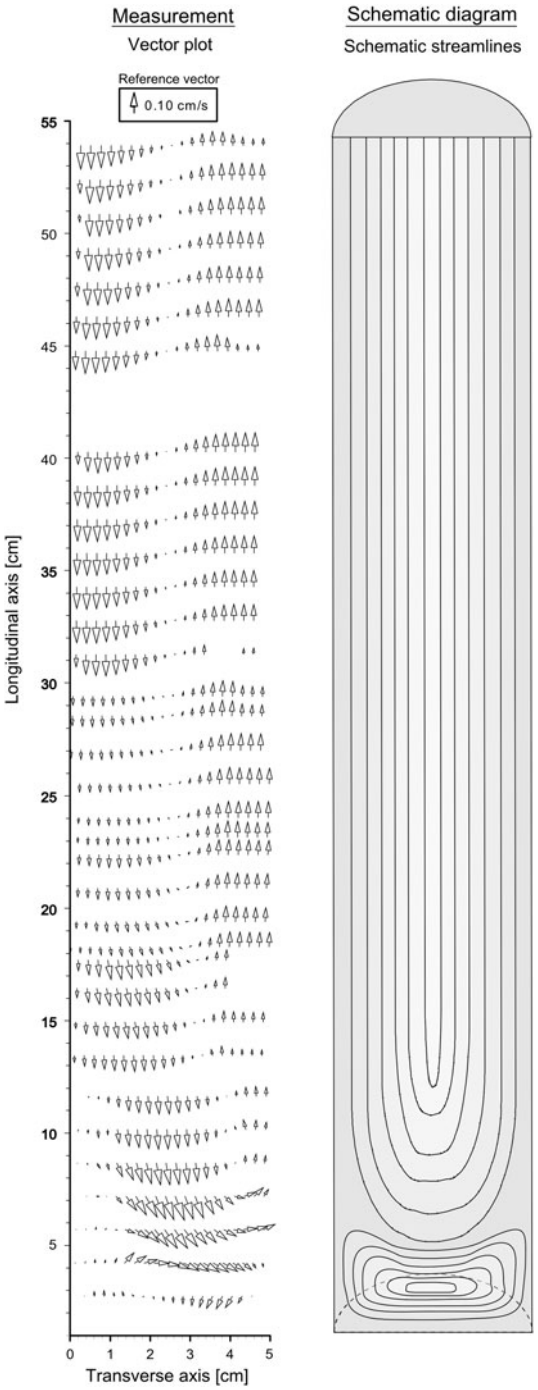

Fig. 7 Flow pattern in the water column reconstructed from PIV measurements at a temperature gradient of 1 K/m and their schematic interpretation

Temperature gradients in that order exist under natural conditions in many monitoring wells and boreholes (Berthold and Börner 2008; Berthold 2010).

For the first critical mode of thermal convection (diametrically antisymmetric mode) in infinite cylinders (length/radius >5) of circular cross-section, Gershuni and Zhukhovitskii (1976) give the following approximation:

Table 2 Flow velocities in the water column of the testing facility depending on the temperature gradient

Temperature gradient (K/m)	Velocity (10^{-4} m/s)	Mean velocity	
		(10^{-4} m/s)	(m/day)
0.0	0.05–0.08	0.06	<1
0.1	0.8–1.0	0.9	8
0.2	3.0–4.0	3.5	30
0.4	2.0–3.4	2.7	23
0.6	5.0–6.0	5.5	48
0.8	7.0–9.0	8.0	69
1.0	9.0–11.0	10.0	95
2.0	6.0–8.0	7.0	60

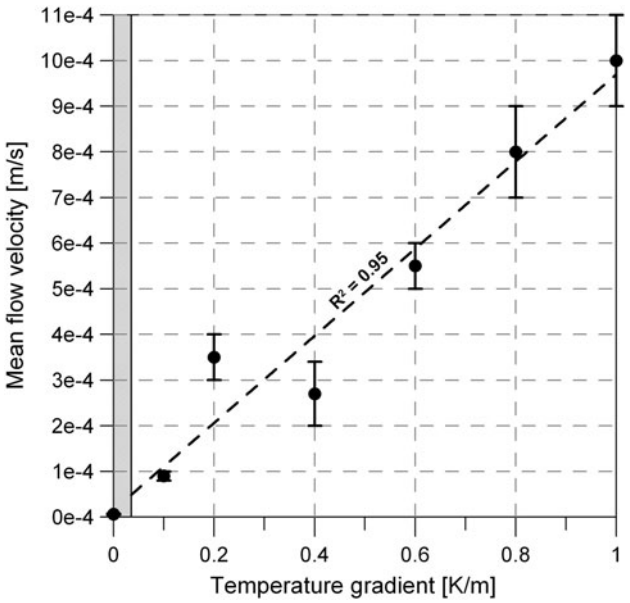

Fig. 8 Mean flow velocity from PIV measurements in the water column at different temperature gradients and linear regression line with coefficient of determination (R^2); the *gray shaded area* indicates the region without thermal convection according to an analytical approximation

$$Ra_{c\,\mathrm{column}} = \frac{96}{5(1+7\tilde{\lambda})}\left[3(33+103\tilde{\lambda}) - \sqrt{3\left(2,567+14,794\tilde{\lambda}+26,927\tilde{\lambda}^2\right)}\right] \quad (2)$$

with $\tilde{\lambda}$ being the ratio between the thermal conductivities of fluid and the surrounding material. The equation was derived for an infinite vertical cylindrical channel surrounded by homogeneous conducting walls under the assumption that the wall temperature is a linear function of the vertical coordinate and that equilibrium temperature gradients in wall and fluid coincide (Gershuni and

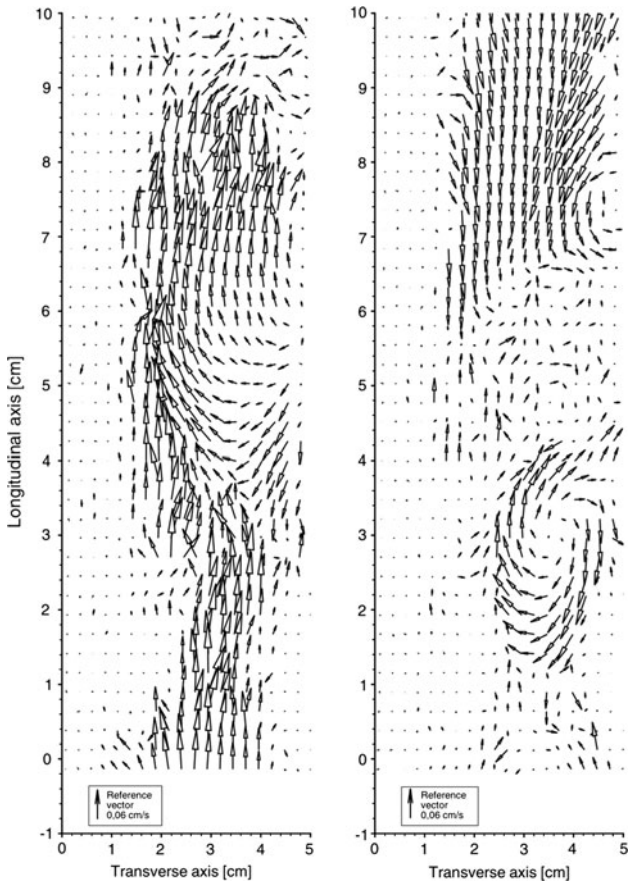

Fig. 9 PIV velocity vector plots of the time-dependent flow at a temperature gradient of 2 K/m—time difference of about 5 min

Zhukhovitskii 1976). They state that the discrepancy between the solution of this approximation and the exact Rayleigh number amounts to a fraction of one percent.

When using a value of 0.6 W/(Km) for water and a thermal conductivity of 2.1 W/(Km) for a surrounding rock formation, a thermal critical Rayleigh number of 147.5 results from their equation. Comparing this critical Rayleigh number with Rayleigh numbers calculated for different water column diameters reveals that in water columns of larger diameters, thermally driven convection sets in at even lower temperature gradients, since friction forces along the wall area are reduced (Fig. 10). For monitoring wells or boreholes with diameters of 7.5 cm (3 inch) and higher that means, they can already experience thermal convection at temperature gradients smaller than the geothermal gradient (Fig. 10).

It is assumed that using the Rayleigh number as a scaling variable, results obtained in this study (e.g., for flow velocities) can be transferred to convective flows in water columns of other diameters. For the experimental parameters in this study, corresponding thermal Rayleigh numbers are given in Table 1.

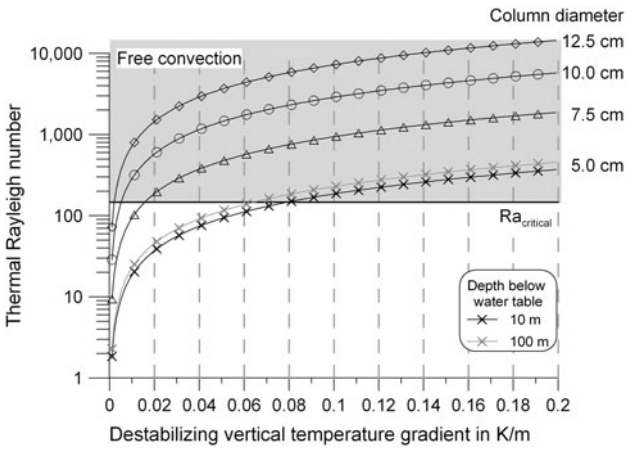

Fig. 10 Rayleigh number as a function of thermal gradient and diameter (temperature: 10°C, water conductivity: 0.3 mS/cm) compared to a critical Rayleigh number for an average rock thermal conductivity of 2.1 W/(Km) and a thermal conductivity of 0.6 W/Km for water

4 Conclusions

Using PIV, thermally driven free convection at low Rayleigh numbers was investigated in a water column subject to small vertical temperature gradients. Depending on the destabilizing gradient, development and geometry of the induced convection cells, as wells as the occurring flow velocities, were determined.

Motivation for the research was to gain more insight into density-driven convection in boreholes and groundwater monitoring wells and study the conditions for their occurrence. The results, however, are not limited to this topic, but apply to a wide range of free convective flow problems.

Temperature gradients in boreholes and groundwater monitoring wells range up to a few Kelvin per meter in the near surface zone, but may also be as small as a few hundredths Kelvin per meter (0.03 K/m on average) due to the geothermal gradient.

Only by using a complicated active and passive insulation system for the testing facility, it was possible to precisely control and maintain the small temperature gradients occurring in boreholes and monitoring wells under natural conditions. An outstanding temperature stability of ± 0.025 K was achieved in the 1-m-long water column. Simulations of free convection in a water column with such a high aspect ratio (height/radius around 19) subject to such precisely controlled small temperature gradients were done for the first time.

The high-precision experimental investigations of thermal convection at low temperature gradients and hence low Rayleigh numbers would not have been possible without PIV. The non-invasive PIV technique allowed for

measuring the resulting low flow velocities with high spatial resolution without interfering the flow.

The experiments revealed that significant free convective flow exists in slender water columns already at considerable low vertical temperature gradients. Regarding the water column in monitoring wells, this was disbelieved before (Martin-Hayden 2001).

In the testing facility representing a 1-m-long section of a water column with 5 cm diameter (approx. 2 inch) within a temperature-stratified medium, occurrence of free convection could be verified for destabilizing temperature gradients from 2 K/m down to 0.1 K/m (smallest adjustable constant temperature gradient). Temperature gradients in that order exist under natural conditions in many monitoring wells and boreholes—the higher ones especially in the near surface zone influenced by seasonal temperature variations.

By proving the existence of thermal convection for temperature gradients down to at least 0.1 K/m ($Ra = 355$), the experiments agree with an analytical approximation of Gershuni and Zhukhovitskii (1976), which proposes that thermal convection should start for a vertical temperature gradient (temperature increasing downwards) of 0.068 K/m in a 5-cm-diameter water column.

The experimental results show an increase in flow velocity with temperature gradient. As regards the quasi-stationary flow regime, the induced flow velocities increased linearly with increasing temperature gradient. Flow velocities ranged from 8×10^{-5} m/s for a temperature gradient of 0.1 K/m ($Ra = 355$) to 1×10^{-3} m/s for a temperature gradient of 1 K/m ($Ra = 3{,}719$).

At higher temperature gradients, a transition was observed (in this case between 1 and 2 K/m, that is, $Ra = 3{,}719$ and 7,812). The quasi-stationary flow, where transport happened mainly over a large convection cell, transformed into a time-dependent flow, where the convection cells changed position within the water column, number, and form temporarily—partly within few minutes.

As the investigated temperature gradients induced convection cells with flow velocities in the order of 10^{-4} m/s, that is, several meters to around hundred meters per day, it results for boreholes and groundwater monitoring wells that the velocity of vertical density-driven convection within the water column can exceed the natural (horizontal) groundwater trough flow.

It is assumed that the flow velocities and structures obtained in this study for density-driven flow in a 5-cm-diameter water column can be transferred to flow velocities in water columns with other diameters using the Rayleigh number as a scaling variable. The results should thus be generally applicable to thermally driven convection in every slender tall water column.

Acknowledgments This study was financed by the German Federal Ministry of Education and Research (BMBF) through the Research Project PTJ-UMW-0330525 under the Project Executive Organization Juelich GmbH (PTJ). We thank Elka Lobutova, Michael Mede, and Helmut Hoppe for fruitful discussion and technical help.

References

Arakeri JH, Avila FE, Dada JM, Tovar RO (2000) Convection in a long vertical tube due to unstable stratification-a new type of turbulent flow? Curr Sci 79(6):859–866

Azouni M (1987) Evolution of non linear flow structure with aspect ratio. Int Comm Heat Mass Transfer 14:447–456

Azouni MA, Normand C (1983) Thermoconvective instabilities in a vertical cylinder of water with maximum density effects—part 1. Exp Geophys Astrophys Fluid Dyn 23:209–222

Barczewski B, Grimm-Strehle J, Bisch G (1993) (Suitability test of groundwater monitoring wells) Überprüfung der Eignung von Grundwasserbeschaffenheitsmessstellen. Wasserwirtschaft 83:72–78

Batchelor GK, Nitsche JM (1993) Instability of stratified fluid in a vertical cylinder. J Fluid Mech 252:419–448

Berthold S (2009) (Geophysical detection of free convection in groundwater monitoring wells and boreholes)—Geophysikalischer Nachweis freier Konvektion in Grundwassermessstellen und Bohrungen. Proceedings of DGFZ e.V., Dissertation, vol 39, Dresden, Germany. ISSN 1430-0176

Berthold S (2010) Synthetic convection log—characterization of vertical transport processes in fluid-filled boreholes. J Appl Geophys 72:20–27

Berthold S, Börner F (2008) Detection of free vertical convection and double-diffusion in groundwater monitoring wells with geophysical borehole measurements. Environ Geol 54:1547–1566

Church EP, Granato EG (1996) Bias in ground-water data caused by well-bore flow in long-screen wells. Ground Water 34:262–273

Elci A, Flach GP, Molz JF (2003) Detrimental effects of natural vertical head gradients on chemical and water level measurements in observation wells: identification and control. J Hydrol 281:70–81

Gershuni G, Zhukhovitskii E (1976) Convective stability of incompressible fluids. Keter Publishing House, Jerusalem

Hales A (1937) Convection currents in geysers. Mon Not R Astron Soc Geophys Suppl 4:122–131

Hutchins SR, Acree SD (2000) Ground water sampling bias observed in shallow conventional wells. Ground Water Mon Remed 20:86–93

Jerschow A (2000) Thermal convection currents in NMR: flow profiles and implications for coherence pathway selection. J Magn Reson 145:125–131

Martin-Hayden JM (2001) Characteristics of thermal instability and mixing within groundwater monitoring wells. In: Geological Society of America Annual Meeting, Boston, Massachusetts

Martin-Hayden JM, Robbins GA (1997) Plume distortion and apparent attenuation due to concentration averaging in monitoring wells. Ground Water 35:339–346

Ostroumov GA (1958) Free convection under the conditions of the internal problem. NACA Technical Memorandum no. 1407

Raffel M, Willert C, Weresley S, Kompenhans J (2007) Particle image velocimetry, a practical guide, 2nd edn. Springer, Berlin

Rayleigh L (1916) On convection currents in a horizontal layer of fluid, when the higher temperature is on the under side. Philos Mag 32:529–546

Sammel EA (1968) Convective flow and its effect on temperature logging in small-diameter wells. Geophysics 33:1004–1012